A Hierarchical Algorithm for Indoor Mobile Robot Localization Using RFID Sensor Fusion

Byoung-Suk Choi, *Student Member, IEEE*, Joon-Woo Lee, *Student Member, IEEE*, Ju-Jang Lee, *Fellow, IEEE*, and Kyoung-Taik Park

***Abstract*—This paper addresses a radio-frequency identification (RFID)-based mobile robot localization which adopts RFID tags distributed in a space. Existing stand-alone RFID systems for mobile robot localization are hampered by many uncertainties. Therefore, we propose a novel algorithm that improves the localization by fusing an RFID system with an ultrasonic sensor system. The proposed system partially removes the uncertainties of RFID systems by using distance data obtained from ultrasonic sensors. We define a global position estimation (GPE) process using an RFID system and a local environment cognition (LEC) process using ultrasonic sensors. Then, a hierarchical localization algorithm is proposed to estimate the position of the mobile robot using both GPE and LEC. Finally, the utility of the proposed algorithm is demonstrated through experiments.**

***Index Terms*—Localization, mobile robot, obstacle estimation, radio-frequency identification (RFID), sensor fusion.**

I. Introduction

The infrastructure for building a sensor network, which is a basic element of the digital ecosystem, is growing rapidly [1], [2]. In recent years, a sensor network without limitations of time, place, and situation has been applied to several areas [3]–[7]. Mobile robots based on sensor networks are a typical example of this application. Mobile robots can offer services using a sensor network that has been built into indoor spaces such as offices, homes, and airports. The sensors and robots that are distributed within a space constitute the digital ecosystem.

It has been predicted that indoor mobile robots will be human-friendly robots that interact with people [8], [9]. To ensure the safety and stability of human–robot interaction, more accurate and precise mobile robot localization systems are essential. The classical localization system for mobile robots uses dead-reckoning sensors such as encoders and gyroscopes [10], [11]. Other systems use some combination of cameras, ultrasonic sensors, and the GPS [12]–[14]. However, the dead-reckoning sensors are subject to accumulation errors that can result in inaccurate performance for cases involving large displacements. The other types of sensors are constrained by environmental factors such as illumination in the case of charge-coupled device (CCD) cameras and outdoor conditions for the GPS. These problems in the classical method translate into uncertainties that diminish the accuracy and precision of mobile robot localization.

In order to reduce these uncertainties, researches have been conducted on the applications of sensor networks for mobile robot localization. Several studies have adopted radio-frequency identification (RFID) technology for sensor networks [15]–[18]. Practical features of RFID technology include the following: 1) storage of location and environment information within RFID tags; 2) classification of information using private identification (ID) codes; 3) convenient approach to information; and 4) robustness under environmental changes. Exploiting these features, we can implement a new forming localization system that can address the deficiencies in conventional localization systems. However, RFID systems suffer from technical limitations not unlike those found in conventional systems.

The target of this research is a mobile robot localization applying RFID technology, which uses distributed RFID tags. We propose a novel algorithm to overcome uncertainties in previous RFID systems for mobile robot localization. We focus on a sensor fusion that uses an RFID system and ultrasonic sensors. Localization using a single sensor system cannot guarantee accuracy due to limitations from the system. Thus, ultrasonic sensors and the RFID system are used to complement one another and compensate for each other's limitations. Therefore, a hierarchical localization system is proposed for efficiently using and integrating data obtained from arbitrary environments from each sensor.

The remainder of this paper is organized as follows. In Section II, we address related works and problems to solve. In Section III, the global position estimation (GPE) process using the RFID system is explained. In Section IV, the local environment cognition (LEC) process using ultrasonic sensors is explained. In Section V, the hierarchical algorithm for mobile robot localization using GPE and LEC is explained. Finally, we conclude this paper in Section VI.

II. Related Works and Research Objectives

A. Localization Based on RFID System

RFID systems have several features and functions that depend on the frequency band, nature of the power source, tags,

Manuscript received January 20, 2009; revised May 22, 2009, September 24, 2009, March 11, 2010, March 25, 2010, and July 29, 2010; accepted November 11, 2010. Date of publication January 31, 2011; date of current version May 13, 2011. This work was supported by the Ministry of Knowledge Economy, Korea, through the Technology Innovation Program.

B.-S. Choi, J.-W. Lee, and J.-J. Lee are with the Department of Electrical Engineering, Korea Advanced Institute of Science and Technology, Daejeon 305-701, Korea (e-mail: bs_choi@kaist.ac.kr; jwl@kaist.ac.kr; jjlee@ee.kaist.ac.kr).

K.-T. Park is with the Nano Fusion Production System Research Division, Korea Institute of Machinery and Materials, Daejeon 305-343, Korea (e-mail: ktpark@kimm.re.kr).

Color versions of one or more of the figures in this paper are available online at http://ieeexplore.ieee.org.

Digital Object Identifier 10.1109/TIE.2011.2109330

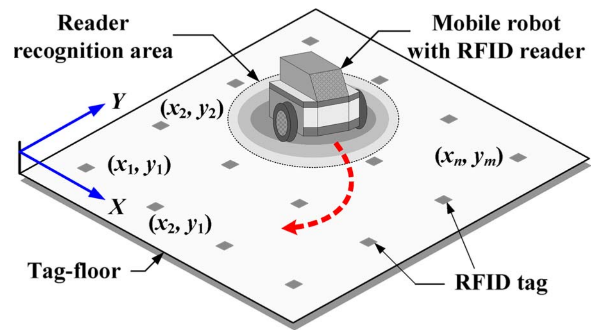

Fig. 1. RFID system based on tag floor for the mobile robot localization, which adopts RFID tags distributed in a space.

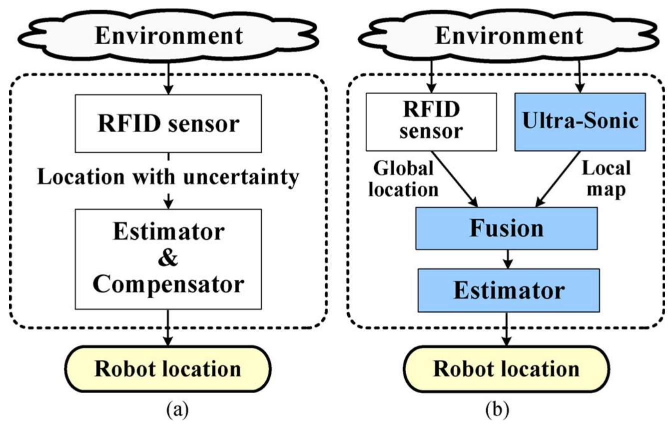

Fig. 2. Differences between the previous system and proposed localization system. (a) Conventional localization system architecture based on RFID technology. (b) Proposed system architecture based on RFID fusion sensor.

etc. Therefore, many localization methods and applications exist in the literature [19]. This paper discusses an RFID system based on a tag floor using passive RFID tags for mobile robot localization, which is addressed in [15] and [20]. Passive RFID tags are arranged in a fixed pattern on the floor, and absolute coordinate values are stored in each tag to provide the position data to the mobile robot, as shown in Fig. 1. An RFID reader (connected to an antenna) is installed underneath the mobile robot for reading the data from the RFID tags. If the robot moves to a position over an RFID tag, the RFID reader reads the coordinate value of the RFID tags to localize the mobile robot. The absolute location of the mobile robot on the floor is estimated without consideration of obstacles or landmarks.

The representative problem of the aforementioned system is that the accurate position and distances between the RFID reader and the RFID tags are not measured. If the RFID tags are found within the reader recognition area, their existence can be just checked. Position estimation errors are thus generated according to the gap between the tags and the reader recognition area. Other problems and uncertainties are fully explained in Section III.

To date, several algorithms have been proposed to solve these problems. Ma and Kim [20] proposed the aforementioned scheme employing a tag arrangement pattern; this method depends on the mobile robot travel path. Hahnel *et al.* [21] and Seo *et al.* [22] used a probabilistic based filter. However, the estimation error increases when no new RFID tags are found. Statistical and probabilistic methods cannot solve the problem rooted in system limitations. In other studies, a triangular arrangement of RFID tags was proposed to reduce the estimation error [23]. However, since this method depends on the gap between the tags, increasing numbers of RFID tags must be used to reduce errors. Further studies examined encoder sensor systems used to compensate for limitations in RFID systems [24]. However, it was found that the error accumulation resulting from wheel slippage may cause the robot to veer off its intended course over long distances. CCD cameras have been used in the fusion system, but these systems are often hampered by illumination problems [25]–[27].

These previous works tried to solve the problem through the temporary exclusion of uncertainties without the direct consideration of the uncertainty associated with RFID systems. Therefore, localization is only efficient in cases where the mobile robot drives along a specific path and for cases where RFID tag information is given continuously.

B. Research Objectives

In this paper, the problems shown in existing studies are considered, and possible solutions are proposed. We present a localization system based on the sensor fusion between an RFID system and ultrasonic sensors. As discussed earlier, the ultrasonic sensors can compensate for the limitations and uncertainties in existing RFID systems. We describe and add a model addressing the uncertainties associated with measurement noise in the RFID system. We assume the mobile robot traveling environment to be a well-structured indoor environment. To reduce the uncertainty associated with measurements from the ultrasonic system, we consider only primitive geometrical objects: straight with regular inclination and circular with regular curvature. We define a GPE process via the RFID system and a LEC process via ultrasonic sensing. We propose a hierarchical localization algorithm to estimate the mobile robot position from GPE and LEC. Fig. 2 highlights the differences between our proposal and the previous work.

III. GPE

A. Uncertainty of RFID System

In Section III, the process of finding the global position of the mobile robot via an RFID system is defined as GPE.

First, we consider the uncertainty of the RFID system when applied for mobile robot localization. The RFID system based on a tag floor estimates the position of the mobile robot through the coordinate value contained in passive RFID tags. Fig. 3 shows the area shaped by the electromagnetic wave from the RFID reader, which is defined as the reader recognition area. If RFID tags exist within the reader recognition area, the RFID tags are activated and can send the ID and coordinate value to the RFID reader. Note that only the existence of RFID tags within the reader recognition area is checked in the RFID system—the distance measurement between the RFID reader and the tags is not available. The uncertainty about the

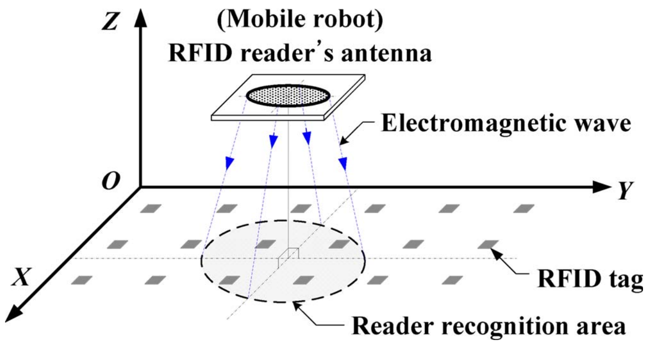

Fig. 3. Shape of electromagnetic wave from RFID reader and recognition area.

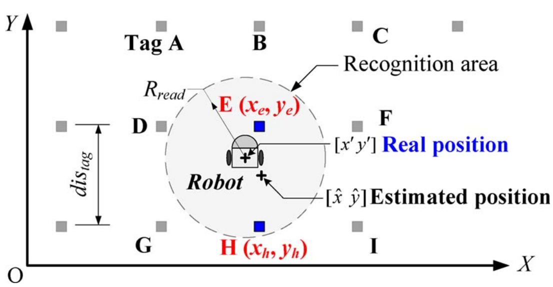

Fig. 4. Uncertainty about position estimation error caused by the reader recognition area.

position estimation error caused by the reader recognition area is represented in Fig. 4. The estimation error is generated by the difference between the actual and the estimated mobile robot position. The position of the mobile robot can be obtained by the RFID tags that are located within the reader recognition area. If same RFID tags are active in spite of the movement of the mobile robot, the estimation position value is not changed. Thus, the tag-floor-based RFID system gives us constrained position data. That is, the mobile robot is considered to be located in the neighborhood of a particular location. Uncertainties about the position measurements can be modeled through the state space and observer function theory.

The estimated state $(\hat{x}(k), \hat{y}(k))$ of the mobile robot at time k is represented as follows:

$$\hat{P}(k) = [\hat{x}(k) \quad \hat{y}(k)]^T = [g_x(z(k)) \quad g_y(z(k))]^T. \tag{1}$$

The observer function G, including the observer data $z(k)$, is defined as follows:

$$G = \begin{bmatrix} g_x(z(k)) \\ g_y(z(k)) \end{bmatrix} = \begin{bmatrix} 0.5(\max\{x_1,\ldots,x_N\} + \min\{x_1,\ldots,x_N\}) \\ 0.5(\max\{y_1,\ldots,y_N\} + \min\{y_1,\ldots,y_N\}) \end{bmatrix} \tag{2}$$

where N represents the number of tags detected by the RFID reader and (x_N, y_N) represents the coordinate value of the RFID tags. We represent the estimated state, including an estimation error, which is caused by the gap between the tags and the reader recognition area

$$\hat{P}(k) = [\hat{x}(k) \quad \hat{y}(k)]^T = [x'(k) + v(k) \quad y'(k) + w(k)]^T \tag{3}$$

where $(x'(k), y'(k))$ is the real position of the mobile robot and $(v(k), w(k))$ is the associated uncertainty. The gap between the tags is dis_{tag}. If the coordinate value stored in tag E is (x_e, y_e), the following equation is obtained:

$$x_e - dis_{\text{tag}} < x'(k) - R_{\text{read}} < x_e$$
$$x_e < x'(k) + R_{\text{read}} < x_e + dis_{\text{tag}}. \tag{4}$$

Using (4), the uncertainty with respect to the X-coordinate and Y-coordinate can be represented as follows:

$$v(k) = |x'(k) - \hat{x}(k)| \leq 0.5|dis_{\text{tag}}|$$
$$w(k) = |y'(k) - \hat{y}(k)| \leq 0.5|dis_{\text{tag}}|. \tag{5}$$

Additionally, we consider the uncertainties about the measurement noise in the RFID system. Real RFID systems are often hampered by some phenomenon such as the time lag of the communication system caused by unspecified reason. This case is regarded as the uncertainty about the measurement noise. At time $k-1$, the estimated state of the mobile robot is represented using (1) and (2). After a sampling period, the estimated state of the mobile robot at time k is shown as follows:

$$\hat{P}(k) = [\hat{x}(k) \quad \hat{y}(k)]^T = [x'(k) + a(k) \quad y'(k) + b(k)]^T. \tag{6}$$

If $\hat{P}(k-1)$ is equal to $\hat{P}(k)$ in spite of the activation of the new RFID tags, the errors $a(k)$ and $b(k)$ represent the uncertainties about the measurement noise and are larger than the uncertainty about the position estimation error caused by the reader recognition area

$$a(k) = |x'(k) - \hat{x}(k-1)| > 0.5|dis_{\text{tag}}|$$
$$b(k) = |y'(k) - \hat{y}(k-1)| > 0.5|dis_{\text{tag}}|. \tag{7}$$

B. GPE of Mobile Robot

Using two uncertainty models, the global position of the mobile robot by the RFID system can be obtained as follows:

$$\hat{P}_G(k) = \begin{bmatrix} \hat{x}(k) \\ \hat{y}(k) \\ \hat{\theta}(k) \end{bmatrix}_G = \begin{bmatrix} x'(k) + a(k) + v(k) \\ y'(k) + b(k) + w(k) \\ \hat{\theta}(k) \end{bmatrix}. \tag{8}$$

The orientation $\hat{\theta}(k)$ of the mobile robot can be estimated using the multiple sets of the estimated global position data as described in [17]. The orientation can be divided into initial orientation and traveling orientation. When the position at time $k = 0$ is denoted as $\hat{P}(0) = [\hat{x}(0) \;\; \hat{y}(0)]^T$ and the position at time $k = 1$ is denoted as $\hat{P}(1) = [\hat{x}(1) \;\; \hat{y}(1)]^T$, the initial orientation of the robot can be obtained as follows:

$$\tan\hat{\theta}(0) = \frac{\hat{y}(1) - \hat{y}(0)}{\hat{x}(1) - \hat{x}(0)} = \frac{d\hat{y}}{d\hat{x}}, \tag{9}$$

$$\hat{\theta}(0) = \tan^{-1}\left(\frac{\hat{y}(1) - \hat{y}(0)}{\hat{x}(1) - \hat{x}(0)}\right) = \tan^{-1}\left(\frac{d\hat{y}}{d\hat{x}}\right). \tag{10}$$

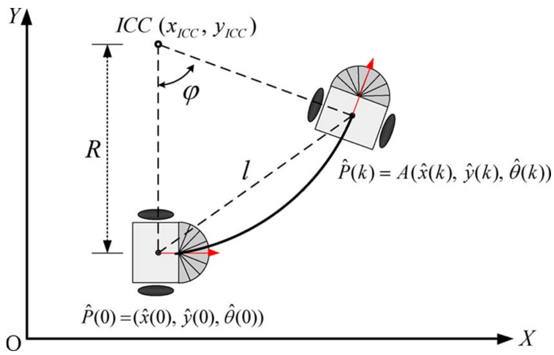

Fig. 5. Orientation estimation of the mobile robot by position of ICC.

Therefore, the initial state of the robot can be represented as a vector with position and orientation as follows:

$$\hat{P}(0) = \begin{bmatrix}\hat{x}(0) & \hat{y}(0) & \hat{\theta}(0)\end{bmatrix}^T = \begin{bmatrix}\hat{x}(0) & \hat{y}(0) & \tan^{-1}(d\hat{y}/d\hat{x})\end{bmatrix}^T. \tag{11}$$

From the initial position and orientation of the mobile robot, the consecutive orientation of the mobile robot is estimated while it is moving. If the mobile robot moves as shown in Fig. 5, the state of the robot can be obtained. Using this information, the rotation radius and angle can be calculated, and the state after the robot movement can be estimated. The orientation of the mobile robot can be obtained by the summation of the initial orientation and the rotation angle as

$$\hat{\theta}(k) = \hat{\theta}(0) + \varphi. \tag{12}$$

Moreover, the rotation radius of the robot R is represented as

$$R = \sqrt{\left(\hat{x}(0) - x_{\mathrm{ICC}}\right)^2 + \left(\hat{y}(0) - y_{\mathrm{ICC}}\right)^2} = \sqrt{\left(\hat{x}(k) - x_{\mathrm{ICC}}\right)^2 + \left(\hat{y}(k) - y_{\mathrm{ICC}}\right)^2}. \tag{13}$$

The ICC is the instantaneous center of curvature of the mobile robot, and the location of the ICC can be determined as

$$\begin{bmatrix} x_{\mathrm{ICC}} \\ y_{\mathrm{ICC}} \end{bmatrix} = \begin{bmatrix} x_{\mathrm{ICC}} \\ -\frac{1}{\tan\left(\hat{\theta}(0)\right)}\left(x_{\mathrm{ICC}} - \hat{x}(0)\right) + \hat{y}(0) \end{bmatrix}. \tag{14}$$

Also, the rotation angle of the robot can be represented

$$\varphi = \cos^{-1}\left(1 - (l^2/2R^2)\right) \tag{15}$$

where $l = \sqrt{(\hat{x}(0) - \hat{x}(k))^2 + (\hat{y}(0) - \hat{y}(k))^2}$.

The traveling orientation can be represented as follows:

$$\hat{\theta}(k) = \hat{\theta}(0) + \cos^{-1}\left(1 - (l^2/2R^2)\right). \tag{16}$$

IV. LEC

A. Uncertainty of Ultrasonic Sensor

The process of recognizing the geometric local area near the mobile robot using ultrasonic sensors is defined as LEC.

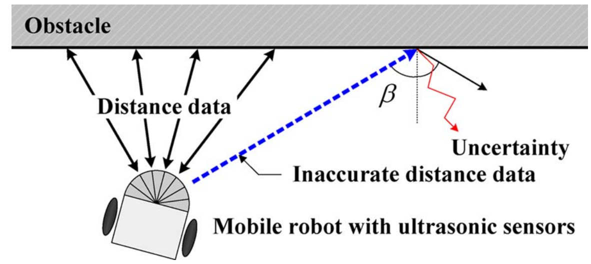

Fig. 6. Principle and uncertainty of ultrasonic sensor in LEC process.

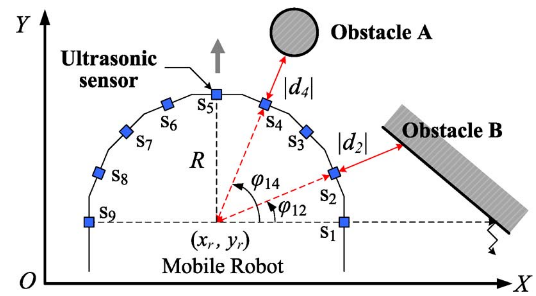

Fig. 7. Platform modeling such as the number and position of sensors in the robot.

Ultrasonic sensors installed in the mobile robot can measure the distance between the mobile robot and the obstacles. However, if the incidence angle or reflection angle β of the sonic beam is large, then accurate distance data cannot be obtained, as shown in Fig. 6. This follows from the exactitude of direction, sensitivity of the reflection angle, and sensitivity of distortion. Also, the radiation angle of the ultrasonic beam is larger when there is more distance between the mobile robot and the obstacle. Therefore, there are uncertainties when using ultrasonic sensors to recognize the local area near the mobile robot. We propose a scheme to reduce these uncertainties in the LEC process.

B. Scheme to Cognize the Local Area

We assume the search space of the mobile robot to be a well-structured indoor environment. In this case, we are able to consider the environmental elements as the straight obstacle with regular inclination and the circular obstacle with regular curvature.

Step 1—Platform Modeling: We assume that the mobile robot encounters obstacles in its path, as shown in Fig. 7. We define the numbers of ultrasonic sensors in the mobile robot to be n and their positions to be s_j starting from the front right-hand side and moving in a counterclockwise direction ($1 \leq j \leq n$). The distance R represents the distance from the center of the mobile robot to the sensors. The angle φ_{ij} represents the sensor placement angle, and each placement angle between two consecutive sensors is defined as α

$$\alpha = 2\pi/(n-1) \tag{17}$$

$$\varphi_{ij} = (j-i)\alpha. \tag{18}$$

The distance for obstacles is thus obtained for every sampling period. Distance data $d_j(k)$ from the ultrasonic sensor s_j at time

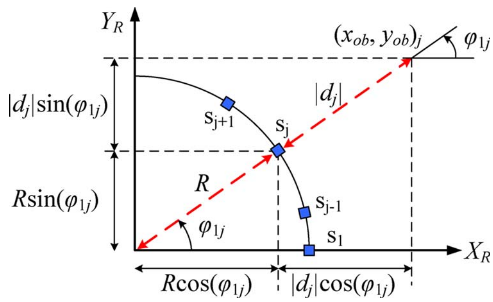

Fig. 8. Geometric modeling by the ultrasonic sensors between the mobile robot and obstacle.

k are shown in Fig. 8. The accuracy of the distance data from the ultrasonic sensor decreases when distances and the incidence angle of the beam for the obstacle are larger. Therefore, the data measured from a beam with a large incidence angle are excluded.

Step 2—Propagation Modeling: The magnitude and direction of the distance vector is defined using measured distance data and sensor location. As shown in Fig. 8, the position of an obstacle as measured by ultrasonic sensor s_j at time k is represented in X–Y robot coordinates

$$\begin{bmatrix} x_{ob}(k) \\ y_{ob}(k) \end{bmatrix}_j = \begin{bmatrix} R\cos\varphi_{1j} + d_j(k)\cos\varphi_{1j} \\ R\sin\varphi_{1j} + d_j(k)\sin\varphi_{1j} \end{bmatrix}. \tag{19}$$

The magnitude and direction of the distance vector for an obstacle is represented as follows:

$$P_{ob}(k)_j = \begin{bmatrix} d_j(k) \\ \theta_{ob}(k) \end{bmatrix} = \begin{bmatrix} \sqrt{x_{ob}^2(k) + y_{ob}^2(k)} \\ \tan^{-1}\left(y_{ob}(k)/x_{ob}(k)\right) \end{bmatrix}. \tag{20}$$

Using the state vector, the position and orientation of the mobile robot at time k are represented as follows:

$$\hat{P}(k) = \begin{bmatrix} \hat{x}(k) & \hat{y}(k) & \hat{\theta}(k) \end{bmatrix}^T. \tag{21}$$

At time $k+1$ after the sampling period, the position of the mobile robot is represented, including the current state and noise

$$\hat{P}(k+1) = H\left(\hat{P}(k), u(k)\right) + e(k). \tag{22}$$

The position and orientation displacement of the mobile robot $u(k)$ are defined using the position and orientation displacement $u(k) = (\Delta x, \Delta y, \Delta\theta)$.

Step 3—Obstacle Estimation Modeling: We assume the surfaces of the obstacles to consist of combinations of linear and curvilinear edges. Under this assumption, the shape of the obstacle is effectively approximated using the distance data. The measurement from the sensors, the robot position, and the geometrical relationship of the environmental elements are depicted in Fig. 9. Through the distance measured at time k, the geometrical position for each element is obtained. The measurement value at time $k+1$ is then obtained according to the movement of the mobile robot.

In detail, the jth sensor location and direction from the robot center to the obstacle at time k is defined as $P_{ob}(k)_j$.

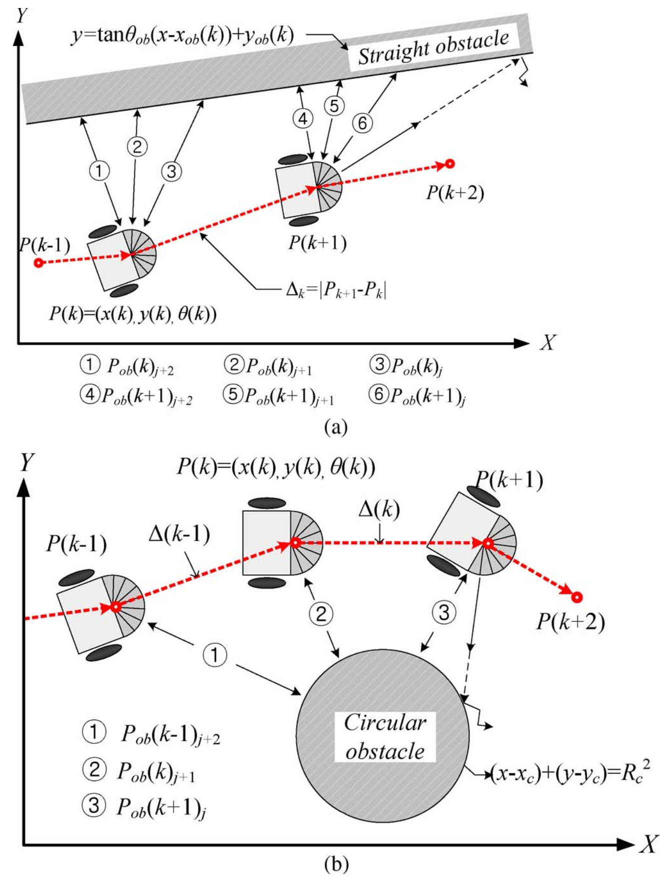

Fig. 9. Obstacle estimation model. (a) Straight obstacle. (b) Circular obstacle.

The obstacle is estimated in connection with the preceding geometrical data about environment elements and data from the propagation of the mobile robot. Geometrical modeling for obstacles with linear edges (i.e., straight obstacle) is presented in Fig. 9(a). Fig. 9(b) shows the modeling for obstacles with curvilinear surfaces (i.e., circular obstacle). The straight and circular obstacles are divided according to the value of curvature as follows [28]:

$$\rho = 1/\lim_{\Delta t\to 0}\left|\frac{\Delta\theta_{ob}}{\Delta t}\right| \quad \left\langle \begin{array}{l} \rho \neq \infty;\ \text{circular obstacle} \\ \rho = \infty;\ \text{straight obstacle.} \end{array} \right. \tag{23}$$

Case I—Straight Obstacle: At the times k and $k+1$, the obstacle states, which are constructed from the jth ultrasonic sensor s_j, are represented as follows:

$$\begin{aligned} P_{ob}(k)_j &= \begin{bmatrix} x_{ob}(k) & y_{ob}(k) & \theta_{ob}(k) \end{bmatrix}_j^T, \qquad 1 \le j \le n \\ P_{ob}(k+1)_j &= \begin{bmatrix} x_{ob}(k+1) & y_{ob}(k+1) & \theta_{ob}(k+1) \end{bmatrix}_j^T \\ &\qquad 1 \le j \le n \end{aligned} \tag{24}$$

where the curvature is infinite for the straight obstacle. Therefore, $\theta_{ob}(k) = \theta_{ob}(k+1)$.

The incidence angle β of the ultrasonic sensor beam for an obstacle is defined as (25), and the state of the obstacle for s_j is only considered if the incidence angle is smaller than γ—this allows us to reduce uncertainties

$$\beta = |\varphi_{1j} + \theta_R - \theta_{ob} - 180^\circ| < \gamma. \tag{25}$$

The obstacle shape is estimated if the following equation is satisfied in order to reduce the error $e(k)$:

$$\min e(k) = \sum_{j=1}^{n} \left(\sqrt{\left(x'_{ob}(k)_j - \hat{x}_{ob}(k)_j\right)^2 + \left(y'_{ob}(k)_j - \hat{y}_{ob}(k)_j\right)^2} \right). \quad (26)$$

The inclination of the straight obstacle is represented as follows:

$$\theta_{ob} = \tan^{-1}\left(\frac{y_{ob}(k+1) - y_{ob}(k)}{x_{ob}(k+1) - x_{ob}(k)}\right). \quad (27)$$

The straight obstacle is represented as follows:

$$y = \tan\theta_{ob}\left(x - x_{ob}(k)\right) + y_{ob}(k). \quad (28)$$

Case II—Circular Obstacle: For circular obstacles, at the times k, $k+1$, and $k+2$, the obstacle states, which are constructed from the jth ultrasonic sensor s_j, are represented as follows:

$$\begin{aligned} P_{ob}(k)_j &= [x_{ob}(k) \quad y_{ob}(k) \quad \theta_{ob}(k)]_j^T, \qquad 1 \le j \le n \\ P_{ob}(k+1)_j &= [x_{ob}(k+1) \quad y_{ob}(k+1) \quad \theta_{ob}(k+1)]_j^T \\ &\qquad 1 \le j \le n \\ P_{ob}(k+2)_j &= [x_{ob}(k+2) \quad y_{ob}(k+2) \quad \theta_{ob}(k+2)]_j^T \\ &\qquad 1 \le j \le n \end{aligned} \quad (29)$$

where the curvature for the circular obstacle is finite and $\theta_{ob}(k) \neq \theta_{ob}(k+1)$. We also consider the state of the obstacle for only j and ultrasonic sensor s_j to satisfy the following condition in order to reduce the error:

$$\beta = |\varphi_{1j} + \theta_R - \theta_{ob} - 180^\circ| < \gamma. \quad (30)$$

Here, the obstacle shape is estimated if the following equation is satisfied in order to reduce the error $e(k)$:

$$\min e(k) = \sum_{j=1}^{n} \left(\sqrt{\left(x'_{ob}(k)_j - \hat{x}_{ob}(k)_j\right)^2 + \left(y'_{ob}(k)_j - \hat{y}_{ob}(k)_j\right)^2} \right). \quad (31)$$

Circular obstacles are represented using the following equations, and the local map is thus obtained:

$$\begin{aligned} &x_{ob}^2(k)_j + y_{ob}^2(k)_j + l x_{ob}(k)_j + m y_{ob}(k)_j + n = 0 \\ &x_{ob}^2(k+1)_j + y_{ob}^2(k+1)_j + l x_{ob}(k+1)_j \\ &\qquad + m y_{ob}(k+1)_j + n = 0 \\ &x_{ob}^2(k+2)_j + y_{ob}^2(k+2)_j + l x_{ob}(k+2)_j \\ &\qquad + m y_{ob}(k+2)_j + n = 0. \end{aligned} \quad (32)$$

The equation of the circular obstacle with the center position and radius is represented as follows:

$$(x - x_c)^2 + (y - y_c)^2 = R_c^2 \quad (33)$$

where (x_c, y_c) is the center of the obstacle and R_c is the radius of the obstacle, respectively.

V. Fusion Algorithm

We estimate the position of the mobile robot through the matching of the aforementioned two data sets. The global position of the mobile robot as obtained from the RFID system is always estimated without reference to any obstacles; however, an estimated error is included as dictated by inherent uncertainties.

On the contrary, the local environment map—which includes the local area of the mobile robot—is partially determined by obstacle distributions. The spread of the obstacles in the real driving environment of the mobile robot is not irregular in spite of the well-structured space. The global position of the mobile robot is considered for basis coordinates because the global position is estimated regardless of the obstacle. Uncertainties in global positioning are then reduced using the local map and data obtained from the mobile robot pertaining to the obstacles. The mobile robot moves continuously, and the flow of the fusion algorithm is depicted using step-by-step instructions.

Step 1. GPE: The observer function of the RFID system is obtained by (2), and then, the global position is estimated in Section III. The uncertainty, (i.e., the estimation error), is included in the estimated global position. The global position can be represented like (8).

Step 2. Mapping of the local environment: When the mobile robot moves within a given global position, a continuous local map is obtained by the movement of the mobile robot. The search area of the ultrasonic sensor is continuously expanded by the movement of the mobile robot. In mapping, the uncertainty is reduced by the matching of the straight and circular obstacles, i.e., (28) and (33), as shown in Section IV.

Step 3. Local position estimation: The local position $\hat{P}_L(k)$ and displacement of the mobile robot are obtained by using the continuous local environment map.

Step 4. Global position compensation: If the GPE does not change in Step 1, we can use the local displacement of the mobile robot for the estimated global position. Because the moving distance and orientation of the mobile robot in an uncertain area of global position are obtained, the technical limitation of the RFID system stated in Section I is solved. In a given global position, the estimation error of the global position is reduced using the local displacement.

Step 5. Final position estimation: Comparing the compensated global position $\hat{P}_G(k)$ from Step 4 and the local position from Step 3, the correspondence of two positions is decided. The set $v(k)$ is defined with the difference

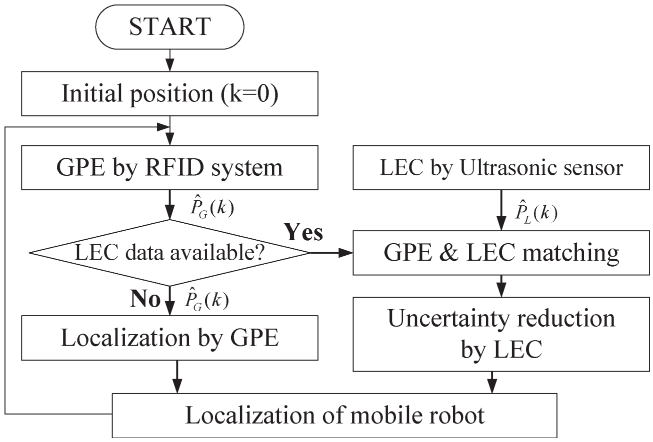

Fig. 10. Flow of the localization of the mobile robot from GPE and LEC.

TABLE I
SYSTEM PARAMETER FOR EXPERIMENTS

Symbol	Quantity	Parameter value
dis_{tag}	Gap between the RFID tags	0.5 m
N	Number of ultrasonic sensors	9
α	Each placement angle between two consecutive sensor	22.5°
γ	Threshold value for incidence angle	60 °
R_{read}	Radius of RFID reader's recognition area	0.3 m

between two values of position, and the covariance matrix $s(k)$ for the difference is represented as follows:

$$v(k) = \left[\hat{P}_G(k) - \hat{P}_L(k)\right] \tag{34}$$

$$S(k) = E\left[v(k)v^T(k)\right]. \tag{35}$$

e is defined as the standard of correspondence and adjusted for the effective corresponding position value from the two position values. Until the difference between two values of position is satisfied, the standard Steps 4 and 5 are repeated

$$v(k)S^{-1}(k)v^T(k) < e^2. \tag{36}$$

Processing for continuous localization is repeated from Steps 1 to 5. This procedure is detailed in Fig. 10.

VI. EXPERIMENTS AND RESULT

In order to verify the proposed algorithm, two experiments were conducted. The estimation error between the real and the estimated robot state was measured. The mobile robot used for the experiments is about 0.3 m $\times$ 0.5 m and is of a car drive type. The RFID reader antenna is installed at the bottom of the robot, and nine ultrasonic sensors are separately installed with a 22.5° angle in front of the robot. The RFID system, KISR300H, is of a passive type and operated at 13.56 MHz. The RFID reader antenna size is 0.15 m $\times$ 0.15 m, and the RFID tags made by epoxy are 0.03 m $\times$ 0.03 m. The ultrasonic sensor module, HRC01, measures the distance to 6 m. The experimental parameters are listed in Table I. The systems used in our experiments are shown in Fig. 11.

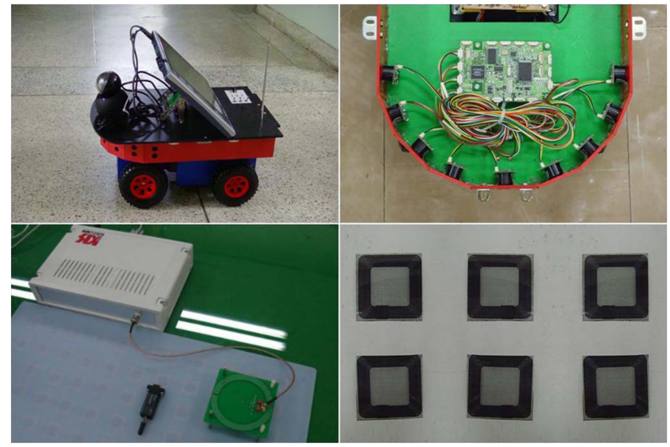

Fig. 11. Mobile robot systems for experiment: Mobile robot, ultrasonic sensor module in front of the mobile robot, RFID reader, and passive RFID tags.

Fig. 12. Corridor environment for the first experiment.

A. Experiment 1

The first experiment had the mobile robot traveling in a corridor as shown in Fig. 12. The RFID tags were set in a rectangular arrangement in the floor, and the coordinate values were stored in advance. The first experiment employed the gap between tags of 0.3 and 0.5 m. In a corridor with a size of 6 m $\times$ 2.4 m, the mobile robot moved from the starting point (5, 142, 0) to the end point (604, 145, 0) for the gap between tags of 0.3 m, and it moved from the starting point (5, 160, 0) to the end point (604, 160, 0) for the gap between tags of 0.5 m. We restricted the maximum velocity of the mobile robot to 0.183 m/s for the real-time process of the localization system. If the mobile robot moves rapidly, the data communication between the RFID reader and the tags sometimes fails. The result data are obtained with a sampling period of 0.25 s.

Three algorithms were used to verify the superiority of the proposed localization systems. The first algorithm introduced in [23] used the coordinate value of the RFID tag as identified by the RFID system. The second algorithm developed in [24] used an RFID system and an encoder system. Fused tag and displacement data were used for the localization. Finally, the third algorithm proposed in this paper used an RFID system and an ultrasonic system.

The first objective of this paper is to find a method to reduce the uncertainty of the basic RFID system. To achieve this goal,

TABLE II
COMPARISON OF AVERAGE ESTIMATION ERROR WITH EACH ALGORITHM

dis_{tag}	Algorithm	Average error
$dis_{tag} = 0.3\ m$	Classic RFID system	25.19 *cm*
	RFID system + Encoder	5.65 *cm*
	Proposed system with algorithm	1.58 *cm*
$dis_{tag} = 0.5\ m$	Classic RFID system	43.41 *cm*
	RFID system + Encoder	10.52 *cm*
	Proposed system with algorithm	2.42 *cm*

we accurately modeled the uncertainty generated in the basic RFID system and proposed the algorithm to reduce the modeled uncertainty through ultrasonic sensors. That is, we regard the proposed system as the extended and improved system from the basic RFID system. The novel localization system supplements the shortcomings of the basic RFID system and yields more improved performance than the basic RFID system. Therefore, the first experiment was conducted in order to compare the performance between the basic RFID system and the proposed system. This is why we used the basic RFID system [23] in the first experiment.

Another objective of this paper is to find a scheme to effectively reduce the uncertainty of the basic RFID system in an indoor environment. In recent works, the encoder or CCD camera is used in order to reduce the uncertainty of the RFID system. The CCD camera or encoder is not effective in a specified environment with a variety of illumination and accumulation errors. We proposed a scheme using the ultrasonic sensor that could be adapted in a general environment. We must show that the proposed novel scheme solves the shortcomings of the CCD camera and encoder. The localization system with the CCD camera and RFID system cannot sometimes estimate the correct position because the CCD camera is easily influenced by the illumination condition. This has been shown in many studies. Therefore, we demonstrated the superiority of our proposed scheme through a comparison with the system using the RFID and encoder system, instead of the system using the CCD camera and RFID system. This is why the previous algorithm [24] using the encoder and RFID system is tested in the first experiment.

From the first algorithm, the position of the mobile robot was obtained by (1)–(5). However, the uncertainties in the basic RFID system were not compensated for because only the coordinate value of the RFID tag was used. The estimation error by uncertainty was determined by (5). Different errors resulted for the cases where the tag gaps were 0.3 and 0.5 m, as shown in Table II and Fig. 13. Also, large errors were sometimes generated in cases where an unforeseen lag occurred. The second algorithm can compensate for the uncertainties associated with the RFID system with the displacement from the encoder. At the early stages in the mobile robot movement, the uncertainty was reduced efficiently. For long traveling distances, however, the uncertainty was not compensated for due to the accumulation error in the encoder. For the third algorithm, the global position was obtained using the RFID system as in the first algorithm. That is, the global position of the mobile robot can be obtained from (8), including the uncertainties in (5) and (7).

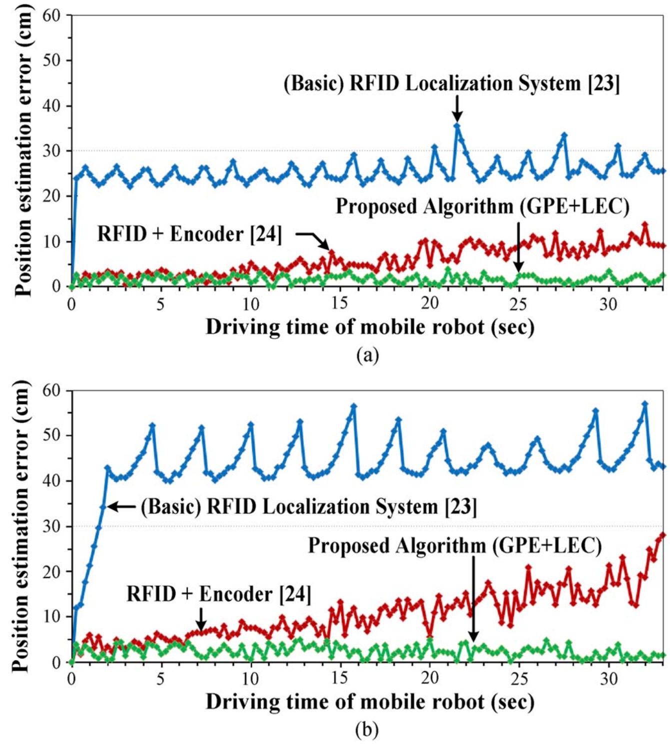

Fig. 13. Results of the first experiment for three algorithms. (a) $dis_{\mathrm{tag}} = 0.3$. (b) $dis_{\mathrm{tag}} = 0.5$.

The uncertainty in RFID system measurements was reduced by the LEC process. Accurate and effective estimation was then possible. The computation times for each algorithm used in the first experiment were 32.2, 44.8, and 47.5 ms, respectively.

B. Experiment 2

The second experiment had the mobile robot traveling in an indoor space populated with straight and circular obstacles as shown in Fig. 14. A constant tag gap of 0.5 m was used. The mobile robot moved from (15, 255, 0) to (10, 35, $-\pi$) along a curved trajectory—the orientation of the robot changed as shown in Fig. 14(b). The maximum velocity of the mobile robot is 0.183 m/s, and the result data are obtained with a sampling period of 0.25 s.

For the comparison of the localization results, the algorithm of Han *et al.* in [15] and our proposed algorithm were used. The algorithm of Han *et al.* [15] only uses an RFID system to obtain the position of the mobile robot. A compensation procedure is included in this algorithm to reduce the uncertainties as given by the RFID system. The motion-continuity property of the differential-driving mobile robot was used in the compensation procedure. This algorithm was affected by the gap between the tags because only the position data obtained from a single RFID system were used. Therefore, when the gap between the tags is large, the compensation procedure is not efficiently realized as shown in Table II—we confirmed this in the result of the experiment.

Using the proposed algorithm, the mobile robot used positional data as in the first experiment. In the initial stage of movement along the path, the distance data obtained by the

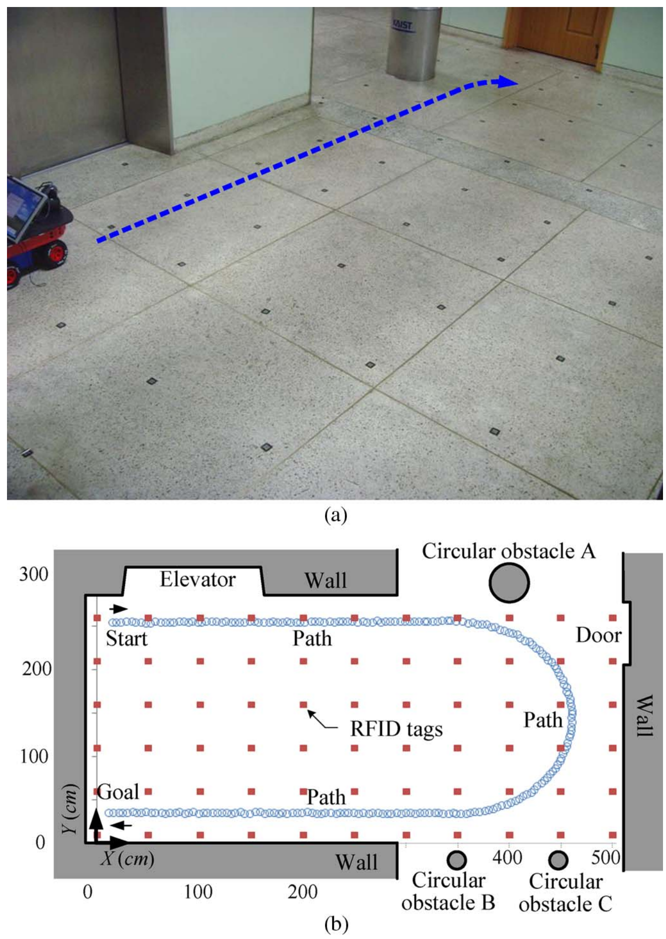

Fig. 14. Second experiment. (a) Environment space. (b) Path of the robot.

straight obstacle—such as the elevator and wall—were used. A local map by the straight obstacle is modeled using (28). It was then used to reduce the uncertainties in the LEC process. In particular, the distance data obtained by the artificial circular obstacle are obtained in the middle stage. By the condition of curvature (23), this obstacle was confirmed to be circular. A local map by the circular obstacle was modeled using (33). As shown in the right of Fig. 14(b), this path included the curve section where the orientation of the robot changes. The orientation of the mobile robot was fixed in the straight path section. Therefore, the orientation estimation was conducted only for the curve section.

The result of the second experiment is shown in Table III. The proposed algorithm can compensate for the positional uncertainties resulting from the RFID system using additional data from the LEC by the obstacle. Therefore, the estimation error could be efficiently reduced in spite of the large gap between the tags. The orientation estimation error was 12.53° using the algorithm proposed in [15], and the orientation estimation error was 7.04° using the algorithm in this paper.

In this experiment, the gap between the tags was 0.5 m. From an economical perspective, the number of RFID tags in a designed space should be minimized—maximum allowable intertag spacing. Note that the estimation error can be reduced effectively using our proposed algorithm even for large tag gaps.

TABLE III
COMPARISON OF SECOND EXPERIMENTAL RESULTS

List	Algorithm	Average error
Position Error	The algorithm of S. Han *et al* in [15]	4.37 *cm*
	Proposed system with algorithm	2.70 *cm*
Orientation Error	The algorithm of S. Han *et al* in [15]	12.53 °
	Proposed system with algorithm	7.04 °

VII. CONCLUSION

This paper has addressed an RFID-based localization scheme for mobile robots which uses ultrasonic sensors to compensate for deficiencies in previous RFID systems. First, two uncertainties of the basic RFID system were modeled. The global position of the mobile robot from the RFID system was obtained in the GPE process. Next, ultrasonic sensors were used for the LEC process. A method to separate straight and circular obstacles was proposed in order to reduce uncertainties in the LEC process. Using a matching algorithm for the global position and the local data, the estimation error and uncertainty were reduced. Experiments verified the effectiveness of our proposed algorithm. The proposed system was able to obtain the position of the mobile robot without any constraint from the environment.

REFERENCES

[1] M. Hadzic and E. Chang, “Application of digital ecosystem design methodology within the health domain,” *IEEE Trans. Syst., Man, Cybern. A, Syst., Humans*, vol. 40, no. 4, pp. 779–788, Jul. 2010.
[2] M. L. Brodie, “Data integration at scale: From relational data integration to information ecosystems,” in *Proc. IEEE Int. Conf. Adv. Inf. Netw. Appl.*, 2010, pp. 2–3.
[3] J. P. Carmo, P. M. Mendes, C. Couto, and J. H. Correia, “A 2.4-GHz CMOS short-range wireless-sensor-network interface for automotive applications,” *IEEE Trans. Ind. Electron.*, vol. 57, no. 5, pp. 1764–1771, May 2010.
[4] K. A. Agha, M.-H. Bertin, T. Dang, A. Guitton, P. Minet, T. Val, and J.-B. Viollet, “Which wireless technology for industrial wireless sensor networks? The development of OCARI technology,” *IEEE Trans. Ind. Electron.*, vol. 56, no. 10, pp. 4266–4278, Oct. 2009.
[5] H.-S. Ahn and K. H. Ko, “Simple pedestrian localization algorithms based on distributed wireless sensor networks,” *IEEE Trans. Ind. Electron.*, vol. 56, no. 10, pp. 4296–4302, Oct. 2009.
[6] V. C. Gungor and G. P. Hancke, “Industrial wireless sensor networks: Challenges, design principles, and technical approaches,” *IEEE Trans. Ind. Electron.*, vol. 56, no. 10, pp. 4258–4265, Oct. 2009.
[7] B. Lu and V. C. Gungor, “Online and remote motor energy monitoring and fault diagnostics using wireless sensor networks,” *IEEE Trans. Ind. Electron.*, vol. 56, no. 11, pp. 4651–4659, Nov. 2009.
[8] C. Mitsantisuk, S. Katsura, and K. Ohishi, “Force control of human–robot interaction using twin direct-drive motor system based on modal space design,” *IEEE Trans. Ind. Electron.*, vol. 57, no. 4, pp. 1383–1392, Apr. 2010.
[9] N. Bu, M. Okamoto, and T. Tsuji, “A hybrid motion classification approach for EMG-based human–robot interfaces using bayesian and neural networks,” *IEEE Trans. Robot.*, vol. 25, no. 3, pp. 502–511, Jun. 2009.
[10] J. Borenstein and L. Feng, “Gyrodometry: A new method for combining data from gyros, and odometry in mobile robots,” in *Proc. IEEE Int. Conf. Robot. Autom.*, 1996, pp. 423–428.
[11] G. Antonelli, S. Chiaverini, and G. Fusco, “A calibration method for odometry of mobile robots based on the least-squares technique: Theory and experimental validation,” *IEEE Trans. Robot.*, vol. 21, no. 5, pp. 994–1004, Oct. 2005.
[12] J. M. Lee, K. Son, M. C. Lee, J. W. Choi, S. H. Han, and M. H. Lee, “Localization of a mobile robot using the image of a moving object,” *IEEE Trans. Ind. Electron.*, vol. 50, no. 3, pp. 612–619, Jun. 2003.

[13] D. Xu, H. Liwei, T. Min, and F. L. You, "Ceiling-based visual positioning for an indoor mobile robot with monocular vision," *IEEE Trans. Ind. Electron.*, vol. 56, no. 5, pp. 1617–1628, May 2009.
[14] B.-S. Choi and J.-J. Lee, "Localization of a mobile robot based on an ultrasonic sensor using dynamic obstacles," *Int. J. Artif. Life Robot.*, vol. 12, no. 1/2, pp. 280–283, Mar. 2008.
[15] S. Han, H. Lim, and J. Lee, "An efficient localization scheme for a differential-driving mobile robot based on RFID system," *IEEE Trans. Ind. Electron.*, vol. 54, no. 6, pp. 3362–3369, Dec. 2007.
[16] R. C. Luo, C.-T. Chuang, and S.-S. Huang, "RFID-based indoor antenna localization system using passive tag and variable RF-attenuation," in *Proc. IEEE Int. Conf. Ind. Electron.*, 2007, pp. 2254–2259.
[17] L. Jing and P. Yang, "A localization algorithm for mobile robots in RFID system," in *Proc. Int. Conf. Wireless Commun., Netw. Mobile Comput.*, 2007, pp. 2109–2112.
[18] K. Kodaka, H. Niwa, Y. Sakamoto, M. Otake, Y. Kanemori, and S. Sugano, "Pose estimation of a mobile robot on a lattice of RFID tags," in *Proc. IEEE/RSJ Int. Conf. Intell. Robot. Syst.*, 2008, pp. 1385–1390.
[19] K. Finkenzeller, *RFID Handbook: Fundamentals and Applications in Contactless Smart Cards and Identification*. Hoboken, NJ: Wiley, 2003.
[20] Y.-K. Ma and S.-W. Kim, "A study on agile navigation system of mess-cleanup robot," in *Proc. Int. Conf. Control, Autom. Syst.*, 2008, pp. 1630–1635.
[21] D. Hahnel, W. Burgard, D. Fox, K. Fishkin, and M. Philipose, "Mapping and localization with RFID technology," in *Proc. IEEE Int. Conf. Robot. Autom.*, 2004, pp. 1015–1020.
[22] D.-S. Seo, H.-G. Lee, H.-S. Kim, G.-W. Yang, and D.-H. Won, "Monte Carlo localization for mobile robots under RFID tag infrastructures," *J. Control Autom. Syst. Eng.*, vol. 12, no. 1, pp. 47–53, Jan. 2006.
[23] B. S. Choi, J. M. Yun, and J. M. Lee, "An efficient localization scheme for an indoor mobile robot," in *Proc. SICE Annual Conf.*, 2005, pp. 2008–2013.
[24] B.-S. Choi, J.-W. Lee, and J.-J. Lee, "Localization and map-building of mobile robot based on RFID sensor fusion system," in *Proc. IEEE Int. Conf. Ind. Informat.*, 2008, pp. 412–417.
[25] H. Chae and K. Han, "Combination of RFID and vision for mobile robot localization," in *Proc. IEEE Int. Conf. Intell. Sens., Sens. Netw., Inf. Proces.*, 2005, pp. 75–80.
[26] B.-S. Choi and J.-J. Lee, "Sensor network based localization algorithm using fusion sensor-agent for indoor service robot," *IEEE Trans. Consum. Electron.*, vol. 56, no. 3, pp. 1457–1465, Aug. 2010.
[27] S. Jia, J. E. Shang, T. Abe, and K. Takase, "Localization of mobile robot with RFID technology and stereo vision," in *Proc. IEEE Int. Conf. Mechatron. Autom.*, 2006, pp. 508–513.
[28] S. Han, B. Choi, and J. Lee, "A precise curved motion planning for a differential driving mobile robot," *Mechatronics*, vol. 18, no. 9, pp. 486–494, Nov. 2008.

Byoung-Suk Choi (S'08) was born in Busan, Korea, in 1981. He received the B.S. and M.S. degrees in electrical engineering from Pusan National University, Busan, in 2004 and 2006, respectively. He is currently working toward the Ph.D. degree at the Korea Advanced Institute of Science and Technology, Daejeon, Korea.

Currently, he is taking part in a research project of the Technology Innovation Program funded by the Ministry of Knowledge Economy, Korea. His research interests include mobile robot and sensor network.

Mr. Choi is a Student Member of the Institute of Control, Robotics and Systems, the Korea Robotics Society, and the Institute of Electronics Engineering of Korea.

Joon-Woo Lee (S'10) was born in Busan, Korea, in 1982. He received the B.S. degree in electrical engineering from Pusan National University, Busan, in 2007, and the M.S. degree in robotics from the Korea Advanced Institute of Science and Technology, Deajeon, Korea, in 2009, where he is currently working toward the Ph.D. degree in electrical engineering.

Currently, he is taking part in a research project of the Technology Innovation Program funded by the Ministry of Knowledge Economy, Korea. His research interests include swarm intelligence and bioinspired robot.

Ju-Jang Lee (M'86–SM'99–F'08) was born in Seoul, Korea, in 1948. He received the B.S. and M.S. degrees in electrical engineering from Seoul National University, Seoul, in 1973 and 1977, respectively, and the Ph.D. degree in electrical engineering from the University of Wisconsin, Madison, in 1984.

From 1977 to 1978, he was a Research Engineer with the Korean Electric Research and Testing Institute, Korea. From 1978 to 1979, he was a Design and Processing Engineer with GTE Automatic Electric Company, North Lake, IL. In 1983, he was briefly the Project Engineer with the Research and Development Department, Wisconsin Electric Power Company, Milwaukee, WI. Since 1984, he has been with the Department of Electrical Engineering and Computer Science, Korea Advanced Institute of Science and Technology, Daejeon, Korea, where he is currently a Professor. In 1987, he was a Visiting Professor at the Robotics Laboratory of Imperial College Science and Technology, London, U.K. From 1991 to 1992, he was a Visiting Scientist at the Robotics of Carnegie Mellon University, Pittsburgh, PA. His current research interests include intelligent control of mobile robot, evolutionary emotional robot, service robot for the disabled, intelligent transportation system, and power system stabilizer. He developed several mobile robots for walking and training and an intelligent bed robotic system for the elderly and disabled. He is an Associate Editor of *Artificial Life and Robotics* and *Machine Intelligence and Robotics Control*. He is an Editor of the *International Journal of Assistive Robotics and Mechatronics*.

Dr. Lee is a Fellow of the Society of Instrument and Control Engineers (SICE) and the Institute of Control, Robotics and Systems. He is an Associate Editor of the IEEE TRANSACTIONS ON INDUSTRIAL ELECTRONICS and the IEEE TRANSACTIONS ON INDUSTRIAL INFORMATICS.

Kyoung-Taik Park was born in Busan, Korea, in 1953. He received the B.S. and M.S. degrees in mechanical engineering from Pusan National University, Busan, in 1977 and 1981, respectively, and the Ph.D. degree in mechanical engineering from the University of Cincinnati, Cincinnati, OH, in 1989.

He is currently with the Nano Fusion Production System Research Division, Korea Institute of Machinery and Materials, Daejeon, Korea. His research interests include robotics, autonomous system, and nanomechatronics.